



Identification of spatiotemporal patterns of biophysical droughts in semi-arid region

B. Kamali et al.

This discussion paper is/has been under review for the journal Hydrology and Earth System Sciences (HESS). Please refer to the corresponding final paper in HESS if available.

Identification of spatiotemporal patterns of biophysical droughts in semi-arid region – a case study of the Karkheh river basin in Iran

B. Kamali¹, K. C. Abbaspour¹, A. Lehmann², B. Wehrli³, and H. Yang^{1,4}

¹Eawag, Swiss Federal Institute of Aquatic Science and Technology, Dübendorf, Switzerland

²EnviroSPACE, Forel Institute for Environmental Science, University of Geneva, Geneva, Switzerland

³Institute of Biogeochemistry and Pollutant Dynamics, ETH Zurich, Switzerland

⁴Department of Environmental Sciences, University of Basel, Basel, Switzerland

Received: 2 February 2015 – Accepted: 8 May 2015 – Published: 3 June 2015

Correspondence to: B. Kamali (bahareh.kamali@eawag.ch)

Published by Copernicus Publications on behalf of the European Geosciences Union.

[Title Page](#)

[Abstract](#)

[Introduction](#)

[Conclusions](#)

[References](#)

[Tables](#)

[Figures](#)

[⏪](#)

[⏩](#)

[◀](#)

[▶](#)

[Back](#)

[Close](#)

[Full Screen / Esc](#)

[Printer-friendly Version](#)

[Interactive Discussion](#)



Abstract

This study aims at identifying historical patterns of meteorological, hydrological, and agricultural (inclusively biophysical) droughts in the Karkheh River Basin (KRB), one of the nine benchmark watersheds of the CGIAR Challenge Program on Water and Food. Standardized precipitation index (SPI), standardized runoff index (SRI), and soil moisture deficit index (SMDI) were used to represent the above three types of droughts, respectively. The three drought indices were compared across temporal and spatial dimensions. Variables required for calculating the indices were obtained from the Soil and Water Assessment Tool (SWAT) constructed for the region. The model was calibrated based on monthly runoff and yearly wheat yield using the Sequential Uncertainty Fitting (SUFI-2) algorithm. Five meteorological drought events were identified in the studied period (1980–2004), of which four corresponded with the hydrological droughts with 1–3 month lag. The meteorological droughts corresponded well with the agricultural droughts during dry months (May–August), while the latter lasted for a longer period of time. Analysis of drought patterns showed that southern parts of the catchment were more prone to agricultural drought, while less influenced by hydrological drought. Our analyses highlighted the necessity for monitoring all three aspects of drought for a more effective watershed management. The analysis on different types of droughts in this study provides a framework for assessing their possible impacts under future climate change in semi-arid areas.

1 Introduction

Drought is a natural and recurrent feature of climate initiated by prolonged dry weather causing less than normal water availability (Tallaksen et al., 2009). It is quantitatively defined in various ways depending on four main perspectives: meteorological, agricultural, hydrological, and socioeconomic drought (Wilhite and Glantz, 1985; Orville, 1990). The first three aspects assess the physical characteristics of this phenomenon,

HESSD

12, 5187–5217, 2015

Identification of spatiotemporal patterns of biophysical droughts in semi-arid region

B. Kamali et al.

[Title Page](#)

[Abstract](#)

[Introduction](#)

[Conclusions](#)

[References](#)

[Tables](#)

[Figures](#)

[⏪](#)

[⏩](#)

[◀](#)

[▶](#)

[Back](#)

[Close](#)

[Full Screen / Esc](#)

[Printer-friendly Version](#)

[Interactive Discussion](#)



and are collectively called biophysical droughts. The socioeconomic drought concerns the water shortfall whose impact ripples through socioeconomic systems (Zdruli et al., 2001).

A common approach for biophysical drought identification is to calculate drought index based on components of land surface cycle (Vidal et al., 2010) and evaluating their spatial and temporal characteristics (McKee et al., 1995; Loukas and Vasiliades, 2004; Vicente-Serrano et al., 2012). The Palmer Drought Severity Index (Palmer, 1965) and the Standardized Precipitation Index (McKee et al., 1993; Edwards and McKee, 1997) are the first generation of drought indices tested worldwide in drought monitoring. Others include rainfall anomaly index (Van-Rooy, 1965), rainfall deciles index (Gibbs and Maher, 1967), reclamation drought index (Weghorst, 1996), surface water supply index (Shafer and Dezman, 1982) and crop-specific drought index (Meyer and Hubbard, 1995).

Most drought indices are calculated based on precipitation as the key variable of water cycle. To better reflect characteristics of drought, some studies have combined different variables to derive more integrative indices including, for example, a copula-based joint deficit index (Kao and Govindaraju, 2010) and a hybrid drought index (Karamouz et al., 2009). There are also studies which have been devoted to assess the propagation of meteorological drought in hydrological or agricultural systems. For example, Hisdal and Tallaksen (2003) carried out a regional assessment of meteorological and hydrological droughts in Denmark. Tallaksen et al. (2009) studied drought propagation through the hydrological cycle by evaluating water deficits in precipitation, groundwater recharge, hydraulic head and discharge in a groundwater fed catchment located in England. Vidal et al. (2010) performed a multi-level analysis of agricultural drought over France and concluded that the ranking of drought events depends highly on both time scale and the variables considered. Tokarczyk and Szalinska (2014) used standardized precipitation index (SPI) and standardized runoff index (SRI) to identify different classes of monthly SPI-SRI indicators using a first-order Markov chain model. They concluded that in Poland, meteorologically dry conditions often shift to hydro-

HESSD

12, 5187–5217, 2015

Identification of spatiotemporal patterns of biophysical droughts in semi-arid region

B. Kamali et al.

[Title Page](#)

[Abstract](#)

[Introduction](#)

[Conclusions](#)

[References](#)

[Tables](#)

[Figures](#)

[⏪](#)

[⏩](#)

[◀](#)

[▶](#)

[Back](#)

[Close](#)

[Full Screen / Esc](#)

[Printer-friendly Version](#)

[Interactive Discussion](#)



Identification of spatiotemporal patterns of biophysical droughts in semi-arid region

B. Kamali et al.

[Title Page](#)

[Abstract](#)

[Introduction](#)

[Conclusions](#)

[References](#)

[Tables](#)

[Figures](#)

[⏪](#)

[⏩](#)

[◀](#)

[▶](#)

[Back](#)

[Close](#)

[Full Screen / Esc](#)

[Printer-friendly Version](#)

[Interactive Discussion](#)

logically dry conditions within the same month, droughts rarely last longer than two months, and two separate drought events can be observed within the same year. Liu et al. (2012) used SPI, SRI and Palmer drought severity index (PDSI) to construct historical drought patterns for the Blue River Basin in Oklahoma and projected the patterns into future using 16 GCM models. They found a good correlation (0.81) between SPI and SRI with a two month lag time. So far, however, few studies have conducted simultaneous drought assessment from meteorological, hydrological, and agricultural perspectives on temporal and spatial dimensions.

In this study, we conduct a comprehensive assessment to fill this lacuna using the Karkheh River Basin (KRB) in Iran as a case study. Our main objectives are to compare meteorological, hydrological, and agricultural droughts represented, respectively, by SPI, SRI, and soil moisture deficit index (SMDI). We explore drought characteristics under different levels of severities; and identify their relationship with crop yield, groundwater recharge and potential evapotranspiration.

KRB is among the nine initial watersheds selected by the Consultative Group on International Agricultural Research (CGIAR) Challenge Program for increasing water productivity of agriculture (Oweis et al., 2009). KRB is known as the food basket of Iran (Ahmad and Giordano, 2010). The importance of analyzing the impact of drought and climate change has been emphasized in many studies (Ashraf Vaghefi et al., 2013a, b; Ahmad and Giordano, 2010; Masih et al., 2010).

2 Materials and methods

2.1 SWAT simulator

To quantify the three aspects of drought, we selected indices obtained from precipitation, runoff, and soil water (SW) content. The data for runoff and SW were derived from a hydrologic model of the KRB developed with the Soil and Water Assessment Tool (SWAT). SWAT is an integrated, semi-distributed, and processed-based hydrologic

Identification of spatiotemporal patterns of biophysical droughts in semi-arid region

B. Kamali et al.

Title Page

Abstract

Introduction

Conclusions

References

Tables

Figures

⏪

⏩

◀

▶

Back

Close

Full Screen / Esc

Printer-friendly Version

Interactive Discussion

model. The model simulates the hydrology of a watershed in two separate components; the land phase and the routing phase. The first phase controls the amount of water, sediment, nutrient and pesticide loadings to the main channel in each catchment, and the second phase defines the movement of water, sediments, nutrients and organic chemicals through the channel network of the watershed to the outlet (Gassman et al., 2007).

SWAT models the local water balance through four storage volumes: snow, soil profile (0–2 m), shallow aquifer (2–20 m) and deep aquifer (> 20 m). The soil water balance equation is the basis of hydrologic modeling. Surface runoff is estimated by a modified Soil Conservation Service-Curve Number (SCS-CN) equation using daily precipitation data and soil hydrologic group, land use and land cover characteristics and antecedent soil moisture. A more detailed description of the model is given by Neitsch et al. (2005). In this study; we used ArcSWAT 2009 with ArcGIS (ESRI-version 9.3).

2.2 Model calibration

The Sequential Uncertainty Fitting Procedure (SUFI-2) was used for model calibration (Abbaspour et al., 2007). The SUFI-2 algorithm for calibration maps all uncertainties on the parameter ranges and tries to capture most of the measured data within the 95% prediction uncertainty. The overall uncertainty in the output is quantified by the 95% prediction uncertainty (95PPU) calculated at the 2.5 and 97.5% levels of cumulative distribution of an output variable obtained through the Latin Hypercube Sampling in the parameters space. The bR^2 (Krause et al., 2005) criterion is used to compare the performance of simulated and observed discharge values expresses as:

$$\varphi = \begin{cases} |b|R^2 & \text{for } |b| \leq 1 \\ |b|^{-1}R^2 & \text{for } |b| > 1 \end{cases} \quad (1)$$

where R^2 is the coefficient of determination and b is the slope of the regression line between the simulated and measured data. The objective function varies between 0 and 1 where 1 indicates a perfect match.

The goodness of fit and the degree to which the calibrated model accounts for the uncertainties are assessed by two indices: r factor and p factor. The p factor is a fraction of measured data bracketed by the 95PPU band. It varies from 0 to 1, where 1 means an ideal 100% bracketing of the measured data. The r factor is the average width of the 95PPU band divided by the standard deviation of the measured variable. A value around 1 is desirable for this parameter (Abbaspour et al., 2009). These two indices can be used to judge the quality of the calibration. A larger p factor can be achieved at the expense of a larger r factor. Hence, often a balance must be reached between the two. When acceptable values of r factor and p factor are reached, then the parameter ranges are the desired parameter distributions representing model uncertainty.

2.3 Drought indices selection

The SPI developed by McKee et al. (1995) and the SRI developed by Shukla and Wood (2008) were selected to monitor meteorological and hydrological droughts, respectively. The agricultural drought is calculated based on the SMDI developed by Narasimhan and Srinivasan (2005).

SPI and SRI indices are computed through fitting probability density functions (to precipitation and runoff, respectively) which are then transformed into the standardized normal distributions. We used a two-parameter Gamma distribution function to calculate the indices as suggested by Lloyd-Hughes and Saunders (2002) and Bordi et al. (2001). Since the indices are normalized, wetter and drier climates can be monitored in the same way and a comparison between different locations can be made (Bordi et al., 2001).

SPI and SRI indices are defined over different time scales (1, 3, 6, 12, 24, and 48 months) and after normalization their values fall between -3 and 3 . Generally,

Identification of spatiotemporal patterns of biophysical droughts in semi-arid region

B. Kamali et al.

Title Page

Abstract

Introduction

Conclusions

References

Tables

Figures

◀

▶

◀

▶

Back

Close

Full Screen / Esc

Printer-friendly Version

Interactive Discussion

smaller time-scales provide early drought warning and its severity, while longer time scales are more indicative of prolonged droughts (Hayes et al., 1997). More details on calculation of SPI and SRI are provided by McKee et al. (1993) and Shukla and Wood (2008).

SMDI was calculated on weekly basis from daily outputs of SWAT for year i and week j based on the soil moisture deficit values ($SD_{i,j}$) calculated as:

$$SD_{i,j} = \begin{cases} \frac{SW_{i,j} - MSW_j}{MSW_j - \min SW_j} \times 100 & \text{if } SW_{i,j} \leq MSW_j \\ \frac{SW_{i,j} - MSW_j}{\max SW_j - MSW_j} \times 100 & \text{if } SW_{i,j} > MSW_j \end{cases} \quad (2)$$

where MSW_j is the long-term (1980–2004) median soil water (mm) for week j , $\min SW_j$ is the long-term minimum available soil water in the soil profile (mm) for week j , $\max SW_j$ is the maximum available soil water in the soil profile (mm) for week j , and $SW_{i,j}$ is the available soil water in the soil profile for week j and year i . In Eq. (2), the seasonality inherent in soil water is removed. Hence, the deficit values can be compared across seasons. SMDI for week j is then expressed as (for details of derivation see Narasimhan and Srinivasan, 2005):

$$SMDI_j = 0.5SMDI_{j-1} + \frac{SD_j}{50} \quad (3)$$

where SMDI during any week will range from -4 to $+4$ representing dry to wet conditions. In order to compare weekly SMDI with monthly SPI and SRI, we considered the values of last week of each month following Narasimhan and Srinivasan (2005). We rescaled the SMDI values from ranges $(-4$ to $4)$ to $(-3$ to $3)$ to be consistent with SPI and SRI values. The four classes of drought indices are then defined consistently for the three indices as: wet (index > 0.75), near normal ($-0.75 < \text{index} < 0.75$), moderate ($-1.5 < \text{index} < -0.75$) and severe (index < -1.5).

Identification of spatiotemporal patterns of biophysical droughts in semi-arid region

B. Kamali et al.

[Title Page](#)

[Abstract](#)

[Introduction](#)

[Conclusions](#)

[References](#)

[Tables](#)

[Figures](#)

[⏪](#)

[⏩](#)

[◀](#)

[▶](#)

[Back](#)

[Close](#)

[Full Screen / Esc](#)

[Printer-friendly Version](#)

[Interactive Discussion](#)



2.4 Study area

KRB covers an area of 51 000 km². It is the third largest basin in Iran. The climate of KRB is mainly semi-arid with annual precipitation ranging from 150 mm in the South to 1000 mm in the North. The basin contains five catchments namely: Gamasiab, Garesu, Seymareh, Kashkan and South Karkheh (hereafter SKarkheh) (Fig. 1). The Karkheh River originates from Gamasiab and then is joined by many streams (Fig. 1). A number of dams have been built on the Karkheh River and many more have been proposed for construction for irrigation and hydropower purposes.

2.5 Data and model set up

Digital Elevation Model (DEM) required by SWAT was obtained from the Shuttle Radar Topography Mission (SRTM by NASA) (Jarvis et al., 2008) with a spatial resolution of 90 m. The global soil map from the Food and Agricultural Organization (FAO) provided data for 5000 soil types comprising two layers (0–30 and 30–100 cm) at the spatial resolution of 10 km (Schuol et al., 2008). Daily climate data including precipitation and temperature in 22 stations (Fig. 1) were obtained from the Iranian Meteorological Organization. The land use map was developed from satellite images (IRS-P6 LISS-IV and IRS-P5-Pan satellite images, ETM+ 2001 Landsat) and 3300 field sampling points by the Iran Water and Power Resources Development Company (2009).

The monthly runoff values of 12 stations and the yearly values of wheat yield in the five catchments obtained from the Iranian Meteorological Organization (Fig. 1) were used for model calibration (1986–2004) and validation (1981–1985).

3 Results

Calibration of the agro-hydrologic model was based on monthly values of river discharges and yearly values of winter wheat yield. For discharge, the p factor were larger than 0.7, meaning, > 70 % of the observed data were bracketed within the prediction

HESSD

12, 5187–5217, 2015

Identification of spatiotemporal patterns of biophysical droughts in semi-arid region

B. Kamali et al.

Title Page

Abstract

Introduction

Conclusions

References

Tables

Figures

⏪

⏩

◀

▶

Back

Close

Full Screen / Esc

Printer-friendly Version

Interactive Discussion



uncertainty of the model. The r factor were mostly around 1, indicating reasonable prediction uncertainties in calibration/verification results (Table 1). The results for annual values of winter wheat yields were similarly good with the exception of larger uncertainty bands in Gamasiab and Seymareh regions (Table 1).

5 Monthly values of precipitation and river discharges and daily values of SW content in 343 subbasins were obtained from SWAT outputs for the period of 1980–2004. From these, we calculated monthly SPI-1, SPI-12, SRI-12 and SMDI indices and aggregated the values for Garesu, Gamasiab, Kashkan, Seymareh and SKarkkeh catchments using weighted areal averages.

10 Comparison of SPI-1 (Fig. 2) and SPI-12 (Fig. 3) shows that drought events did not correspond in the same way for shorter (1 month) and longer (12 months) time scales. For example, in early 1987, the severe to moderate droughts in SPI-1 were in contrast to the near normal situation in SPI-12 in all the catchments. At shorter time scales, droughts show a higher frequency than at longer time scales (Fig. 4). The duration of both moderate and severe drought periods changed noticeably as a function of time scale. At the time scale of 1 month, the longest duration of severe droughts was 7 months, while it was 40 months for SPI-12 (Fig. 4). As drought is better recognized by its persistency (Kumar et al., 2012), we used SPI-12 to represent a meteorological drought in the ensuing analyses.

20 SPI-12 (Fig. 3) highlighted five meteorological drought events (MD1 to MD5). Event MD1 started at late 1983 with moderate severity and lasted until late 1984 for Garesu, Gamasiab, and Kashkan. Seymareh experienced severe drought in 1984, and SKarkkeh's moderate drought persisted until 1986 with short periods of two severe droughts. Event MD2 had higher severity and longer persistency for Garesu, Gamasiab, and Kashkan, while Seymareh and SKarkkeh experienced less severe droughts. MD2 event started in 1989 and lasted until late 1991 in all catchments. The two subsequent events MD3 and MD4 of shorter duration occurred in all catchments. The mega drought event of 1999 MD5 was the last but the most important event of the region. In 2000, the whole basin was in severe drought situation. While Garesu and

HESSD

12, 5187–5217, 2015

Identification of spatiotemporal patterns of biophysical droughts in semi-arid region

B. Kamali et al.

Title Page

Abstract

Introduction

Conclusions

References

Tables

Figures

◀

▶

◀

▶

Back

Close

Full Screen / Esc

Printer-friendly Version

Interactive Discussion

Gamasiab recovered after 2001, moderate to severe droughts lasted for Seymareh and SKarkhe until 2004.

SRI in the KRB was quite similar to SPI in terms of timing and severity of droughts (Fig. 5). We also observed a 3 months lag from SPI-12, indicating that the hydrological drought did not initiate until 3 month after the meteorological drought. All meteorological droughts were successfully captured by hydrological droughts, although HD5 appears more severe and continuous than MD5. HD5 had the most hydrologic consequences in KRB during 1999–2000. The severe meteorological drought MD5 in SKarkheh did not show significant impact on hydrological systems in 2003 (HD5).

We calculated the correlation coefficient of SPI and SRI for four time scales (1, 3, 6 and 12 months) (Table 3). The meteorological droughts were better correlated with hydrological droughts of longer time periods. For example, SRI-1 is mostly correlated with SPI-3. The correlation coefficients equaled 0.77 in Garesu, 0.78 in Gamasiab and Seymareh and 0.63 in SKarkheh. Similarly, SRI-3 and SRI-6 were most correlated with SPI-6 and SPI-12, respectively. As observed before, this suggests a 3-months lag of hydrological response to meteorological droughts. The SPI and SRI correlations in different catchments show higher values for Garesu, Gamasiab and Kashkan (upper basin) and lower values for SKarkheh (lower basin).

The agricultural droughts (SMDI) showed a slightly different picture of the drought history in KRB. In general, there is a much larger variability in the monthly values as compared with SPI (Fig. 6). The frequency of SMDI droughts and intermittent wet periods is higher with shorter duration. Many moderate droughts of early 1980s are not captured by SPI and SRI. This could be due to higher temperature in these years leading to higher evapotranspiration and lower soil moisture. This is corroborated with the below average non-irrigated wheat yield shown by the green line in Fig. 6. The yield line was calculated as relative change in wheat yield (%) by using $[(\text{Actual Yield} - \text{Mean Yield}) \times 100 / \text{Actual Yield}]$. For the Mean Yield we used the 25 year average yield. The yield loss is generally consistent with SMDI. The first agricultural drought (AD1) was most serious in Seymareh and SKarkheh. The drought of 1985 in SKarkheh is

HESSD

12, 5187–5217, 2015

Identification of spatiotemporal patterns of biophysical droughts in semi-arid region

B. Kamali et al.

Title Page

Abstract

Introduction

Conclusions

References

Tables

Figures

◀

▶

◀

▶

Back

Close

Full Screen / Esc

Printer-friendly Version

Interactive Discussion



HESSD

12, 5187–5217, 2015

Identification of spatiotemporal patterns of biophysical droughts in semi-arid region

B. Kamali et al.

[Title Page](#)

[Abstract](#)

[Introduction](#)

[Conclusions](#)

[References](#)

[Tables](#)

[Figures](#)

[⏪](#)

[⏩](#)

[◀](#)

[▶](#)

[Back](#)

[Close](#)

[Full Screen / Esc](#)

[Printer-friendly Version](#)

[Interactive Discussion](#)

not depicted by SRI-12, but SPI-12 indicates moderate to severe drought for this year. The most drought discrepancy in drought indices between SMDI and SPI and SRI is in the period of 1986 to 1989. While the latter two show normal to wet conditions, severe to moderate droughts are observed based on SMDI, especially in SKarkheh where persistent drought extends to 2004. The drought period AD2 matches the MD2 of SPI-12. For this period, SRI-12 is not in agreement with the other two indices. Lack of rainfall during MD2 has been reflected in agricultural drought by substantially lowering the wheat yield. The severely insufficient rainfall in the second half of 1991 in Gamasiab and Kashkan resulted in moderate SRI values. The third SPI drought did not cause any SMDI drought in late 1995, but the fourth moderate SPI drought, MD4, expressed itself as moderate SRI and mostly severe SMDI drought in the entire KRB catchment. Finally, the prolonged drought of 1999–2004 was indicated as moderate to severe drought by all indices. Up to 100 % wheat failure was observed in SKarkheh, which is the most drought-vulnerable region in KRB.

A correlation between monthly SMDI and yearly wheat yields indicated largest values during May–August (Fig. 7). Phenologically, this is in the reproductive stage of wheat development, where crop is most susceptible to water stress.

The characteristics of the three types of droughts are quantitatively defined with respect to severity, duration, start, end, and affected area for the three types of droughts in Table 4. Here we only reported on droughts covering more than 25 % of spatial extent or longer than two months in duration. The severity ranges of affected areas are obtained from the 343 subbasins modelled in SWAT. Clearly, from the five identified meteorological drought events only four influenced the hydrological sectors. Event AD3 influenced soil water content in dry months of 1996. Hydrological sector responds with 1–3 months lag time with less severity and shorter duration. Agricultural drought events persisted for longer period e.g. MD2 lasted 22 months, but AD2 lasted 26 months.

4 Discussion

4.1 Temporal characteristics of meteorological drought indices

Comparison of SPI-1 and SPI-12 showed that droughts have different frequencies and duration according to the time scale used for analysis. At shorter time scales, the duration of dry periods was short, but with higher frequency; at longer time scales, persistent drought with lower frequency were better identified. Shorter time scales could be used to infer early drought warning. This is important as soil moisture and consequently vegetation activity respond predominantly to short scales.

On the other hand, due to long-term development and duration of drought, the progressive characters of drought impacts are only apparent after a long period of precipitation deficit (Vicente-Serrano and Lopez-Moreno, 2005). It is difficult to identify periods of consecutive dry conditions in shorter time scales, as the higher frequency of SPI at the shorter time scales could hide important dry periods. Therefore, it is necessary to analyze the longer time scales to identify the main dry periods.

Generally, comparing different time scales of SPI is necessary to fully analyze drought situations, as the most appropriate time scale can regionally vary due to rain-fall pattern. Our analysis regarding the role of different time scales in KRB showed the highest correlation of SRIs with SPI-12. This is in agreement with the study by Vicente-Serrano and Lopez-Moreno (2005) which suggested that SPI longer than 12 month time scale may not be useful for drought identifications. Other studies showed time scales of 3 to 12 months to be best, depending on climatic situation of the region (Xu et al., 2011; Hayes et al., 1999).

Our results show that the correlation between SPI-1 and SPI-3, 6, 9 and 12 (Table 2) decreases with increasing time scale. This is consistent with Narasimhan and Srinivasan (2005), which showed that the correlation between SPI-1, and SPI-3,6,9, and 12 decreased from 0.6 (with SPI-3) to 0.26 with (SPI-12). Similar results were also found in Liu et al. (2012) for Oklahoma, Duan and Mei, (2014) for the Huai River Basin in China, and Wang et al. (2011) for central Illinois.

Identification of spatiotemporal patterns of biophysical droughts in semi-arid region

B. Kamali et al.

[Title Page](#)

[Abstract](#)

[Introduction](#)

[Conclusions](#)

[References](#)

[Tables](#)

[Figures](#)

[⏪](#)

[⏩](#)

[◀](#)

[▶](#)

[Back](#)

[Close](#)

[Full Screen / Esc](#)

[Printer-friendly Version](#)

[Interactive Discussion](#)



4.2 Comparison of the three drought indices

We have used the two most widely used drought indices (SPI and SRI) in combination with SMDI (on weekly based) for drought monitoring. The three indices with the aid of SWAT model provided the possibility to capture major drought events in three aspects. The time series of SPI-12 identified five meteorological drought events experienced during 1980–2004 (MD1–MD5) from which four corresponded with hydrological droughts (HD1,2,4,5). HD3 had insignificant consequence in hydrological and agricultural sectors.

The correlation between SPI-12 and SRI-12 showed the highest value. This is consistent with the work of Liu et al. (2012) who reported a correlation of 0.81. SRI showed similar patterns with SPI but with a 3 months lag (Figs. 3 and 5). However, our results did not show the situation as reported by Tokarczyk and Szalinska (2014) in Poland where meteorologically dry conditions often shift to hydrologically dry conditions within the same month, and that droughts rarely last longer than two months. This may be because of very different climatic and hydrological conditions in KRB and the basin studied in Poland.

Several factors may cause the 3 month lag seen in hydrological response to rainfall deficit. One is that the hydrologic drought is linked not only to precipitation, but also to rain intercept, soil infiltration, evapotranspiration, and groundwater flow. Depending on basin properties (such as soil type, land use and topography), quick-responding and slow-responding catchments are formed, leading to different groundwater and then stream flow responses.

The lag in the occurrence of SRI drought in Garesu, Gamasiab and Kashkan catchments is mostly due to being infiltration-dominated catchments. This is indicated by the larger groundwater recharge in these catchments (Fig. 8a) as compared with Seymareh and SKarkkeh. The increase in recharge during March–May is mostly due to increased snow melt in these mountainous regions. The lag in Seymareh and SKarkkeh catchments is, however, caused by a different mechanism. The flow in these down-

Identification of spatiotemporal patterns of biophysical droughts in semi-arid region

B. Kamali et al.

[Title Page](#)

[Abstract](#)

[Introduction](#)

[Conclusions](#)

[References](#)

[Tables](#)

[Figures](#)

[⏪](#)

[⏩](#)

[◀](#)

[▶](#)

[Back](#)

[Close](#)

[Full Screen / Esc](#)

[Printer-friendly Version](#)

[Interactive Discussion](#)



stream catchments is dominated by a mixed-flow regime fed by regional flow from local precipitation as well as runoff from upstream catchments.

For example, the runoff from Garesu and Gamasiab are discharged into the streams that contribute directly to runoff in Seymareh. This leads to differences in timing and severity of meteorological and hydrological droughts in Seymareh and SKarkheh. The severe meteorological drought in 2003 in SKarkheh did not show as hydrological drought in the upper catchments. The lower values for correlation coefficient of 3 month lag between SPIs and SRI in the southern catchments are probably the results of such mixed-flow regimes.

Agricultural drought was identified using SMDI obtained from soil moisture. Soil moisture has an important impact on drought development because any reduction in soil moisture content causes low actual evapotranspiration, resulting in low biomass. Considering soil moisture as a drought index is more relevant in catchments with semi-arid climates because of high evapotranspiration (Fig. 8b). Within such climate, the precipitation is mostly insufficient to replenish the soil moisture. Soil moisture reaches the wilt-point in almost all years. Consequently, the variation in potential evapotranspiration can hardly affect the actual evapotranspiration. Therefore, actual evapotranspiration is strongly controlled by precipitation and soil moisture in catchments with semi-arid climate.

The comparison of the patterns of SMDI with SPI-12 indicates that SMDI corresponded to the meteorological droughts MD1 to MD5; but it did not capture the severity, duration, and frequency of droughts. The major reason is that apart from rainfall, the increasing temperatures and accelerating evaporative demands lead to a progressive drying of the soil, decreased actual evapotranspiration, and eventually yield loss.

Our findings showed that, in general, when the recovery of soil moisture took longer time, the catchment experienced consecutive agricultural drought conditions. Supplemental irrigation is recommended for increasing crop yield and water productivity in such areas with intense agricultural activities.

Identification of spatiotemporal patterns of biophysical droughts in semi-arid region

B. Kamali et al.

Title Page

Abstract

Introduction

Conclusions

References

Tables

Figures

◀

▶

◀

▶

Back

Close

Full Screen / Esc

Printer-friendly Version

Interactive Discussion



Although we did not directly assess the economic drought in this study, the economic impact of agricultural drought has been partially reflected by wheat yield loss. Our findings confirmed that the SWAT model was able to capture yield anomalies that were observed during drought situations. Based on these relationships, it is possible to also quantify the impact of meteorological and hydrological droughts in terms of losses to ecosystem flow, environmental services, and watershed-scale restoration programs.

5 Conclusion

This study analyzed the 25 year historical droughts of different catchments in KRB at different time-scales. We used SPI, SRI and SMDI to assess drought conditions. The hydrological model SWAT was used to simulate soil moisture at different temporal resolutions and to calculate soil moisture deficit index. Such approach integrates hydrological parameters of soil type and land cover as well as meteorological parameters which provides more in depth understanding of agricultural droughts.

Five meteorological drought events were identified in the studied period (1980–2004), of which four corresponded with the hydrological droughts with 1–3 month lag. The meteorological droughts corresponded well with the agricultural droughts during dry months (May–August), while the latter lasted for a longer period of time. SMDI corresponded to the meteorological drought periods MD1 to MD5; but showed different severity, duration, and frequency of droughts.

We concluded that the set of drought indices developed in this study constitutes a versatile tool that can be used in an operational context for drought monitoring and provides a broader understanding of drought impact on different water sectors.

Identification of spatiotemporal patterns of biophysical droughts in semi-arid region

B. Kamali et al.

[Title Page](#)

[Abstract](#)

[Introduction](#)

[Conclusions](#)

[References](#)

[Tables](#)

[Figures](#)

[⏪](#)

[⏩](#)

[◀](#)

[▶](#)

[Back](#)

[Close](#)

[Full Screen / Esc](#)

[Printer-friendly Version](#)

[Interactive Discussion](#)



References

- Abbaspour, K. C., Yang, J., Maximov, I., Siber, R., Bogner, K., Mieleitner, J., Zobrist, J., and Srinivasan, R.: Modelling hydrology and water quality in the pre-ailpine/alpine Thur watershed using SWAT, *J. Hydrol.*, 333, 413–430, doi:10.1016/j.jhydrol.2006.09.014, 2007.
- 5 Abbaspour, K. C., Faramarzi, M., Ghasemi, S. S., and Yang, H.: Assessing the impact of climate change on water resources in Iran, *Water Resour. Res.*, 45, W10434, doi:10.1029/2008wr007615, 2009.
- Ahmad, M. U. D. and Giordano, M.: The Karkheh River basin: the food basket of Iran under pressure, *Water Int.*, 35, 522–544, doi:10.1080/02508060.2010.510326, 2010.
- 10 Ashraf Vaghefi, S., Mousavi, S. J., Abbaspour, K. C., Srinivasan, R., and Arnold, J. R.: Integration of hydrologic and water allocation models in basin-scale water resources management considering crop pattern and climate change: Karkheh River Basin in Iran, *Reg. Environ. Change*, 15, 475–484, doi:10.1007/s10113-013-0573-9, 2013a.
- Ashraf Vaghefi, S., Mousavi, S. J., Abbaspour, K. C., Srinivasan, R., and Hong, Y.: Analyses of the impact of climate change on water resources components, drought and wheat yield in semiarid regions: Karkheh River Basin in Iran, *Hydrol. Process.*, 28, 2018–2032, 2013b.
- 15 Bordi, I., Frigio, S., Parenti, P., Speranza, A., and Sutera, A.: The analysis of the Standardized Precipitation Index in the Mediterranean area: large-scale patterns, *Ann. Geofis.*, 44, 965–978, 2001.
- 20 Duan, K. and Mei, Y.: Comparison of meteorological, hydrological, and agricultural drought responses to climate change and uncertainty assessment, *Water Resour. Manage.*, 28, 5039–5054, 2014.
- Edwards, D. C. and McKee, T. B.: Characteristics of 20th century drought in the United States at multiple time scales, Colorado State Univ., Ft. Collins, CO, 1997.
- 25 Gassman, P. W., Reyes, M. R., Green, C. H., and Arnold, J. G.: The soil and water assessment tool: historical development, applications, and future research directions, *T. ASABE*, 50, 1211–1250, 2007.
- Gibbs, W. J. and Maher, J. V.: Rainfall deciles as drought indicators, Commonwealth of Australia, Melbourne, Australia, 1967.
- 30 Hayes, M., Svoboda, M., Wilhite, D., and Vanyarkho, O.: Monitoring the 1996 drought using the Standardized Precipitation Index, 10th Conference on Applied Climatology, Bulletin of the

Identification of spatiotemporal patterns of biophysical droughts in semi-arid region

B. Kamali et al.

Title Page

Abstract

Introduction

Conclusions

References

Tables

Figures

◀

▶

◀

▶

Back

Close

Full Screen / Esc

Printer-friendly Version

Interactive Discussion



HESSD

12, 5187–5217, 2015

Identification of spatiotemporal patterns of biophysical droughts in semi-arid region

B. Kamali et al.

[Title Page](#)[Abstract](#)[Introduction](#)[Conclusions](#)[References](#)[Tables](#)[Figures](#)[⏪](#)[⏩](#)[◀](#)[▶](#)[Back](#)[Close](#)[Full Screen / Esc](#)[Printer-friendly Version](#)[Interactive Discussion](#)

American Meteorological Society, National Drought Mitigation Center, Lincoln, Nebraska, 190–191, 1997.

Hayes, M. J., Svoboda, M. D., Wilhite, D. A., and Vanyarkho, O. V.: Monitoring the 1996 drought using the standardized precipitation index, *B. Am. Meteorol. Soc.*, 80, 429–438, doi:10.1175/1520-0477(1999)080<0429:Mtduts>2.0.Co;2, 1999.

Hisdal, H. and Tallaksen, L. M.: Estimation of regional meteorological and hydrological drought characteristics: a case study for Denmark, *J. Hydrol.*, 281, 230–247, doi:10.1016/S0022-1694(03)00233-6, 2003.

Jarvis, A., Reuter, H. I., Nelson, A., and Guevera, E.: Hole-filled SRTM for the globe Version 4, the CGIAR-CSI SRTM 90 m Database, available at: <http://srtm.csi.cgiar.org> (last access: January 2013), 2008.

Kao, S. C. and Govindaraju, R. S.: A copula-based joint deficit index for droughts, *J. Hydrol.*, 380, 121–134, doi:10.1016/j.jhydrol.2009.10.029, 2010.

Karamouz, M., Rasouli, K., and Nazif, S.: Development of a hybrid index for drought prediction: case study, *J. Hydrol. Eng.*, 14, 617–627, doi:10.1061/(Asce)He.1943-5584.0000022, 2009.

Krause, P., Boyle, D. P., and Bäse, F.: Comparison of different efficiency criteria for hydrological model assessment, *Adv. Geosci.*, 5, 89–97, doi:10.5194/adgeo-5-89-2005, 2005.

Kumar, M. N., Murthy, C. S., Sai, M. V. R. S., and Roy, P. S.: Spatiotemporal analysis of meteorological drought variability in the Indian region using standardized precipitation index, *Meteorol. Appl.*, 19, 256–264, doi:10.1002/Met.277, 2012.

Liu, L., Yang, H., and Bednarczyk, C. N.: Hydro-climatological drought analyses and projections using meteorological and hydrological drought indices: a case study in Blue River Basin, Oklahoma, *Water Resour. Manage.*, 26, 2761–2779, 2012.

Lloyd-Hughes, B. and Saunders, M. A.: A drought climatology for Europe, *Int. J. Climatol.*, 22, 1571–1592, doi:10.1002/Joc.846, 2002.

Loukas, A. and Vasiliades, L.: Probabilistic analysis of drought spatiotemporal characteristics inThessaly region, Greece, *Nat. Hazards Earth Syst. Sci.*, 4, 719–731, doi:10.5194/nhess-4-719-2004, 2004.

Masih, I., Uhlenbrook, S., Maskey, S., and Ahmad, M. D.: Regionalization of a conceptual rainfall–runoff model based on similarity of the flow duration curve: a case study from the semi-arid Karkheh basin, Iran, *J. Hydrol.*, 391, 190–203, doi:10.1016/j.jhydrol.2010.07.018, 2010.

Identification of spatiotemporal patterns of biophysical droughts in semi-arid region

B. Kamali et al.

[Title Page](#)

[Abstract](#)

[Introduction](#)

[Conclusions](#)

[References](#)

[Tables](#)

[Figures](#)

[⏪](#)

[⏩](#)

[◀](#)

[▶](#)

[Back](#)

[Close](#)

[Full Screen / Esc](#)

[Printer-friendly Version](#)

[Interactive Discussion](#)

- McKee, T. B., Doesken, N. J., and Kleist, J.: The Relationship of Drought Frequency and Duration to Time Scales, Eighth Conference on Appl. Clim., Anaheim, California, 17–22 January 1993.
- McKee, T. B., Doesken, N. J., and Kleist, J.: Drought monitoring with multiple time scales, Ninth Conference on Appl. Clim., Dallas, Texas, 233–236, 1995.
- Meyer, S. J. and Hubbard, K. G.: Extending the crop-specific drought index to soybean, Ninth Conference on Appl. Clim., Dallas, Texas, 258–259, 1995.
- Narasimhan, B. and Srinivasan, R.: Development and evaluation of Soil Moisture Deficit Index (SMDI) and Evapotranspiration Deficit Index (ETDI) for agricultural drought monitoring, *Agr. Forest Meteorol.*, 133, 69–88, doi:10.1016/j.agrformet.2005.07.012, 2005.
- Neitsch, S. L., Arnold, J. G., Kiniry, J. R., Williams, J. R., and King, K. W.: Soil and Water Assessment Tool. Theoretical documentation: Version 2009, TWRITR-191, Texas Water Resources Institute, College Station, TX, 2005.
- Orville, H. D.: Ams statement on meteorological drought, *B. Am. Meteorol. Soc.*, 71, 1021–1023, 1990.
- Oweis, T., Siadat, H., and Abbasi, F.: Improving On-farm Agricultural Water Productivity in the Karkheh River Basin (KRB) in: CPWF Project Report-Project Number 08, CGIAR Challenge Program on Water and Food, Colombo, Sri Lanka, 2009.
- Palmer, W. C.: Meteorological drought, US Weather Bureau, NOAA Library and Information Services Division, Washington, D.C., 1965.
- Schulz, J., Abbaspour, K. C., Yang, H., Srinivasan, R., and Zehnder, A. J. B.: Modeling blue and green water availability in Africa, *Water Resour. Res.*, 44, W07406, doi:10.1029/2007wr006609, 2008.
- Shafer, B. A. and Dezman, L. E.: Development of a Surface Water Supply Index (SWSI) to Assess the Severity of Drought Conditions in Snowpack Runoff Areas, *Western SnowConf.*, Reno, Nevada, 1982.
- Shukla, S. and Wood, A. W.: Use of a standardized runoff index for characterizing hydrologic drought, *Geophys. Res. Lett.*, 35, L02405, doi:10.1029/2007gl032487, 2008.
- Tallaksen, L. M., Hisdal, H., and Van Lanen, H. A. J.: Space–time modelling of catchment scale drought characteristics, *J. Hydrol.*, 375, 363–372, doi:10.1016/j.jhydrol.2009.06.032, 2009.
- Tokarczyk, T. and Szalinska, W.: Combined analysis of precipitation and water deficit for drought hazard assessment, *Hydrolog. Sci. J.*, 59, 1675–1689, 2014.

Identification of spatiotemporal patterns of biophysical droughts in semi-arid region

B. Kamali et al.

[Title Page](#)

[Abstract](#)

[Introduction](#)

[Conclusions](#)

[References](#)

[Tables](#)

[Figures](#)

[⏪](#)

[⏩](#)

[◀](#)

[▶](#)

[Back](#)

[Close](#)

[Full Screen / Esc](#)

[Printer-friendly Version](#)

[Interactive Discussion](#)



Van-Rooy, M. P.: A Rainfall Anomaly Index (RAI) independent of time and space, *Notos*, 14, 43–48, 1965.

Vicente-Serrano, S. M. and López-Moreno, J. I.: Hydrological response to different time scales of climatological drought: an evaluation of the Standardized Precipitation Index in a mountainous Mediterranean basin, *Hydrol. Earth Syst. Sci.*, 9, 523–533, doi:10.5194/hess-9-523-2005, 2005.

Vicente-Serrano, S. M., Begueria, S., Gimeno, L., Eklundh, L., Giuliani, G., Weston, D., El Kenawy, A., Lopez-Moreno, J. I., Nieto, R., Ayenew, T., Konte, D., Ardo, J., and Pegram, G. G. S.: Challenges for drought mitigation in Africa: the potential use of geospatial data and drought information systems, *Appl. Geogr.*, 34, 471–486, doi:10.1016/j.apgeog.2012.02.001, 2012.

Vidal, J.-P., Martin, E., Franchistéguy, L., Habets, F., Soubeyroux, J.-M., Blanchard, M., and Baillon, M.: Multilevel and multiscale drought reanalysis over France with the Safran-Isba-Modcou hydrometeorological suite, *Hydrol. Earth Syst. Sci.*, 14, 459–478, doi:10.5194/hess-14-459-2010, 2010.

Wang, D., Hezaji, M., Cai, X., and Valocchi, A. J.: Climate change impact on meteorological, agricultural, and hydrological drought in central Illinois, *Water Res. Res.*, 47, W09527, doi:10.1029/2010WR009845, 2011.

Weghorst, K. M.: *The Reclamation Drought Index: Guidelines and Practical Applications*, Bureau of Reclamation, Denver, CO, 6 pp., 1996.

Wilhite, D. A. and Glantz, M. H.: Understanding the drought phenomenon: the role of definitions, *Water Int.*, 10, 111–120, 1985.

Xu, Y. P., Lin, S. J., Huang, Y., Zhang, Q. Q., and Ran, Q. H.: Drought analysis using multi-scale standardized precipitation index in the Han River Basin, China, *J. Zhejiang Univ.-Sc. A*, 12, 483–494, doi:10.1631/jzus.A1000450, 2011.

Zdruli, P., Jones, R. J. A., and Montanarella, L.: Use of soil and climate data to assess the risk of agricultural drought for policy support in Europe, *Agronomie*, 21, 45–56, 2001.

Identification of spatiotemporal patterns of biophysical droughts in semi-arid region

B. Kamali et al.

[Title Page](#)

[Abstract](#)

[Introduction](#)

[Conclusions](#)

[References](#)

[Tables](#)

[Figures](#)

[⏪](#)

[⏩](#)

[◀](#)

[▶](#)

[Back](#)

[Close](#)

[Full Screen / Esc](#)

[Printer-friendly Version](#)

[Interactive Discussion](#)

Table 1. Calibration (1986–2004) and validation (1980–1985) performances of simulated runoff and wheat yield in SWAT based on br_2 , p factor and r factor values in the five catchments.

Runoff Catchments	Calibration		bR2	Verification		bR2
	p factor	r factor		p factor	r factor	
Gamasiab	0.70	1.02	0.50	0.65	1.30	0.55
Garesu	0.65	1.04	0.65	0.60	1.25	0.70
Kashkan	0.80	0.89	0.80	0.78	1.35	0.65
Seymareh	0.81	1.20	0.70	0.65	1.15	0.61
SKarkheh	0.83	1.17	0.70	0.75	1.12	0.63
Wheat Yield						
Gamasiab	0.78	2.1	0.78	0.66	1.9	0.8
Garesu	0.76	1.2	0.74	0.75	1.4	0.7
Kashkan	0.80	1.39	0.89	0.60	1.4	0.78
Seymareh	0.67	2.45	0.7	0.70	1.93	0.81
SKarkheh	0.56	0.82	0.63	0.58	1.01	0.58

Identification of spatiotemporal patterns of biophysical droughts in semi-arid region

B. Kamali et al.

Table 2. Cross-correlation between different time scales of SPI (3–24 months) in Garesu and Skarkkeh subbasins.

		SPI-1	SPI-3	SPI-6	SPI-9	SPI-1	SPI-2
Garesu	SPI-1	1	0.69	0.40	0.31	0.29	0.10
	SPI-3		1	0.58	0.44	0.36	0.14
	SPI-6			1	0.75	0.64	0.28
	SPI-9				1	0.86	0.43
	SPI-1					1	0.53
	SPI-2						1
SKarkkeh	SPI-1	1.00	0.69	0.39	0.34	0.27	0.20
	SPI-3		1.00	0.55	0.49	0.37	0.28
	SPI-6			1.00	0.72	0.61	0.42
	SPI-9				1.00	0.82	0.49
	SPI-1					1.00	0.55
	SPI-2						1.00

Title Page

Abstract

Introduction

Conclusions

References

Tables

Figures

◀

▶

◀

▶

Back

Close

Full Screen / Esc

Printer-friendly Version

Interactive Discussion

Identification of spatiotemporal patterns of biophysical droughts in semi-arid region

B. Kamali et al.

Title Page

Abstract

Introduction

Conclusions

References

Tables

Figures

◀

▶

◀

▶

Back

Close

Full Screen / Esc

Printer-friendly Version

Interactive Discussion

Table 3. Correlation coefficient of SPI with SRI in different time scales and in the five catchments; the highest correlation values of SRIs with SPIs are written bold.

		SRI-1	SRI-3	SRI-6	SRI-12
Garesu	SPI-1	0.30	0.15	0.10	0.08
	SPI-3	0.77	0.51	0.31	0.22
	SPI-6	0.73	0.77	0.72	0.44
	SPI-12	0.72	0.76	0.79	0.82
Gamasiab	SPI-1	0.30	0.11	0.04	0.04
	SPI-3	0.78	0.45	0.20	0.12
	SPI-6	0.64	0.74	0.64	0.34
	SPI-12	0.70	0.73	0.74	0.75
Kashkan	SPI-1	0.35	0.23	0.12	0.08
	SPI-3	0.87	0.51	0.29	0.13
	SPI-6	0.54	0.86	0.71	0.38
	SPI-12	0.62	0.60	0.77	0.82
Seymareh	SPI-1	0.37	0.17	0.08	0.06
	SPI-3	0.78	0.56	0.31	0.19
	SPI-6	0.71	0.79	0.72	0.41
	SPI-12	0.68	0.74	0.76	0.80
SKarkheh	SPI-1	0.43	0.19	0.06	0.06
	SPI-3	0.63	0.36	0.36	0.23
	SPI-6	0.58	0.59	0.62	0.49
	SPI-12	0.47	0.44	0.66	0.60

Identification of spatiotemporal patterns of biophysical droughts in semi-arid region

B. Kamali et al.

[Title Page](#)

[Abstract](#)

[Introduction](#)

[Conclusions](#)

[References](#)

[Tables](#)

[Figures](#)

[◀](#)

[▶](#)

[◀](#)

[▶](#)

[Back](#)

[Close](#)

[Full Screen / Esc](#)

[Printer-friendly Version](#)

[Interactive Discussion](#)

Table 4. The characteristics of meteorological, hydrological and agricultural drought events identified in KRB, the severity and affected area were presented in terms of maximum and minimum ranges from 95 percentiles.

Index	Event	Severity range	Months in droughts	Start	End (%)	Affected area
Meteorological drought	MD1	[−1.70, −0.8]	18 months	Oct 1983	Mar 1986	[26 %, 97 %]
	MD2	[−2.0, −0.80]	22 months	Oct 1989	Nov 1991	[42 %, 91 %]
	MD3	[−2.3, −0.85]	3 months	Nov 1995	Jan 1996	[60 %, 92 %]
	MD4	[−1.3, −0.76]	7 months	Apr 1997	Oct 1997	[51 %, 80 %]
	MD5	[−2.3, −0.91]	37 months	Mar 1999	Nov 2003	[45 %, 100 %]
Hydrologic drought	HD1	[−2.1, −0.8]	14 months	Mar 1984	Mar 1986	[37 %, 85 %]
	HD2	[−1.5, −0.8]	12 months	Mar 1991	Feb 1992	[49 %, 70 %]
	HD3	No hydrological drought is found				
	HD4	[−1.7, −0.8]	11 months	May 1997	Mar 1998	[32 %, 58 %]
	HD5	[−2.3, −0.9]	33 months	Apr 1999	Oct 2003	[32 %, 93 %]
Agricultural drought	AD1	[−2.48, −0.8]	20 months	Oct 1983	Apr 1986	[31 %, 77 %]
	AD2	[−2.45, −0.9]	26 months	Apr 1989	Dec 1991	[37 %, 93 %]
	AD3	[−2.1, −1]	3 months	May 1996	Aug 1996	[30 %, 80 %]
	AD4	[−2.8, −0.93]	9 months	May 1997	Apr 1998	[34 %, 100 %]
	AD5	[−2.5, −0.93]	45 months	May 1999	Oct 2004	[42 %, 92 %]

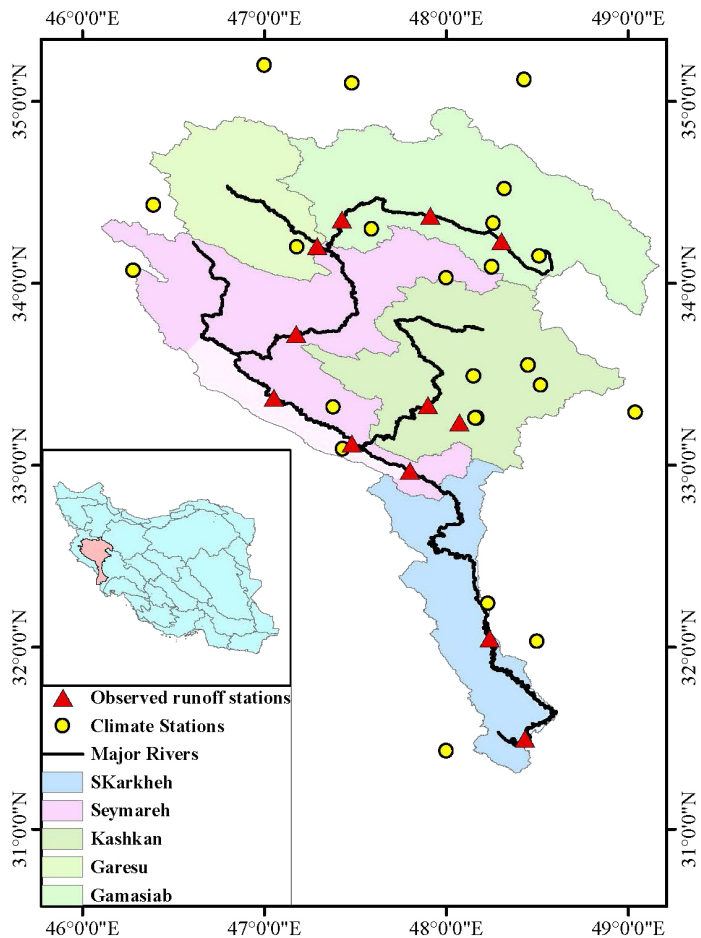


Figure 1. The Karkheh River Basin and the five major catchments; the major river and its tributaries, the 22 climate stations and 12 observed runoff outlets used in calibration.

Identification of spatiotemporal patterns of biophysical droughts in semi-arid region

B. Kamali et al.

[Title Page](#)

[Abstract](#)

[Introduction](#)

[Conclusions](#)

[References](#)

[Tables](#)

[Figures](#)

[◀](#)

[▶](#)

[◀](#)

[▶](#)

[Back](#)

[Close](#)

[Full Screen / Esc](#)

[Printer-friendly Version](#)

[Interactive Discussion](#)

Identification of spatiotemporal patterns of biophysical droughts in semi-arid region

B. Kamali et al.

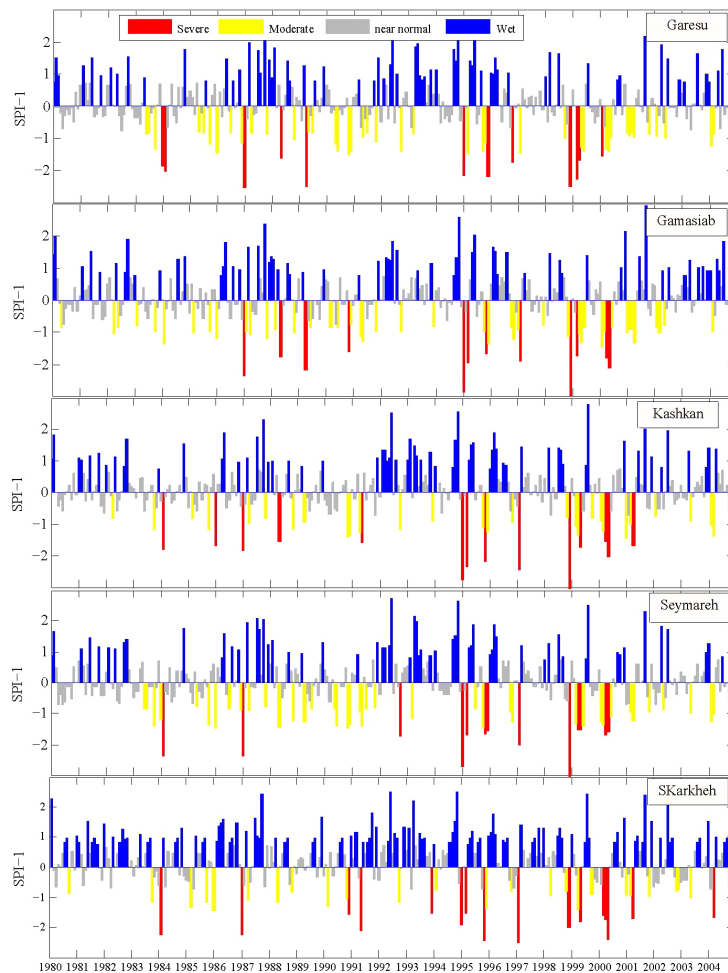


Figure 2. The time series of SPI-1 in the five catchments of KRB during the period 1980–2004.

[Title Page](#)[Abstract](#)[Introduction](#)[Conclusions](#)[References](#)[Tables](#)[Figures](#)[◀](#)[▶](#)[◀](#)[▶](#)[Back](#)[Close](#)[Full Screen / Esc](#)[Printer-friendly Version](#)[Interactive Discussion](#)

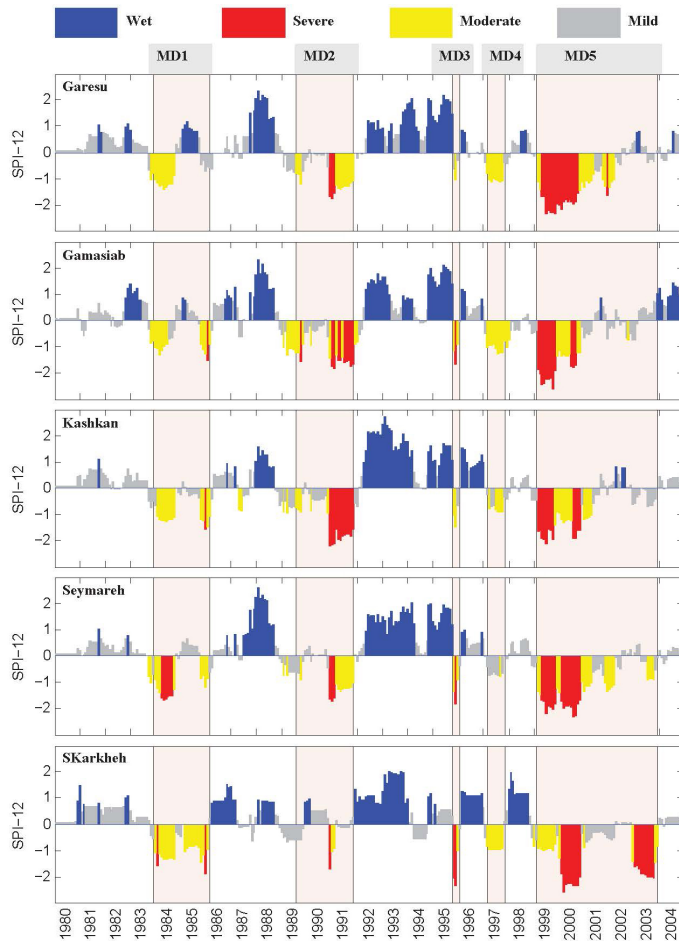


Figure 3. The time series of SPI-12 in the five catchments of KRB during the period 1980–2004; The shaded bars highlight the five meteorological drought events (MD1–MD5).

Identification of spatiotemporal patterns of biophysical droughts in semi-arid region

B. Kamali et al.

[Title Page](#)

[Abstract](#)

[Introduction](#)

[Conclusions](#)

[References](#)

[Tables](#)

[Figures](#)

[⏪](#)

[⏩](#)

[◀](#)

[▶](#)

[Back](#)

[Close](#)

[Full Screen / Esc](#)

[Printer-friendly Version](#)

[Interactive Discussion](#)

Identification of spatiotemporal patterns of biophysical droughts in semi-arid region

B. Kamali et al.

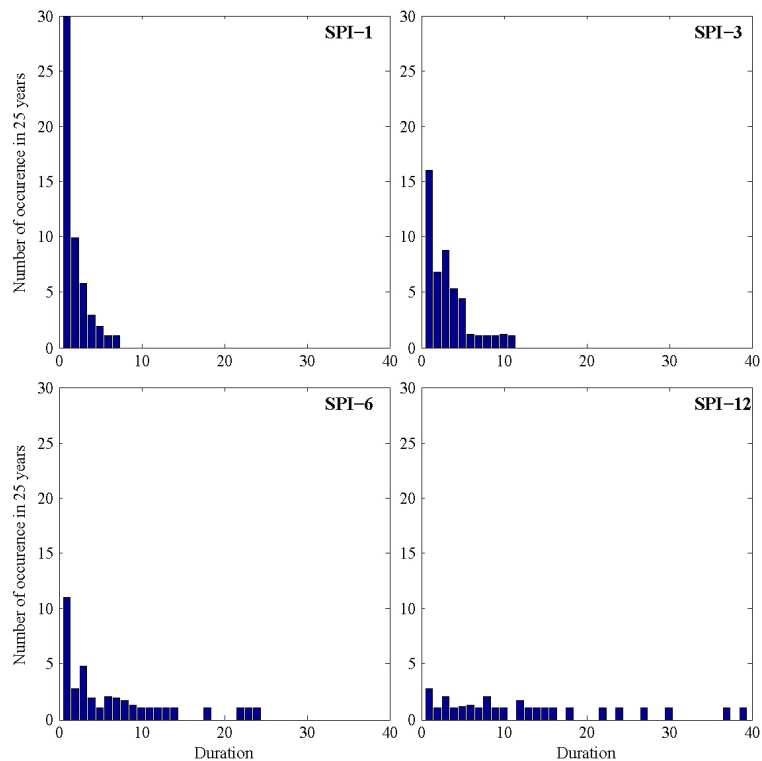


Figure 4. The relations between duration of drought and number of occurrences in four time scales (1, 3, 6, 12) of SPI.

[Title Page](#)[Abstract](#)[Introduction](#)[Conclusions](#)[References](#)[Tables](#)[Figures](#)[⏪](#)[⏩](#)[◀](#)[▶](#)[Back](#)[Close](#)[Full Screen / Esc](#)[Printer-friendly Version](#)[Interactive Discussion](#)

Identification of spatiotemporal patterns of biophysical droughts in semi-arid region

B. Kamali et al.

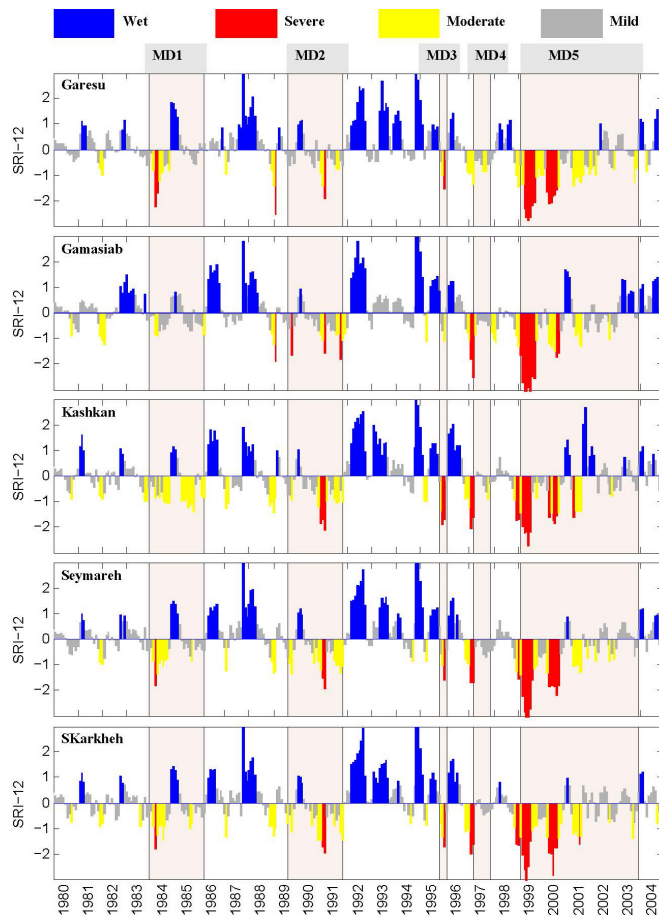


Figure 5. The time series of SRI-12 index in the five catchments of KRB during the period 1980–2004; The shaded bars highlight the five hydrological drought events (HD1–HD5).

Title Page

Abstract

Introduction

Conclusions

References

Tables

Figures

◀

▶

◀

▶

Back

Close

Full Screen / Esc

Printer-friendly Version

Interactive Discussion

Identification of spatiotemporal patterns of biophysical droughts in semi-arid region

B. Kamali et al.

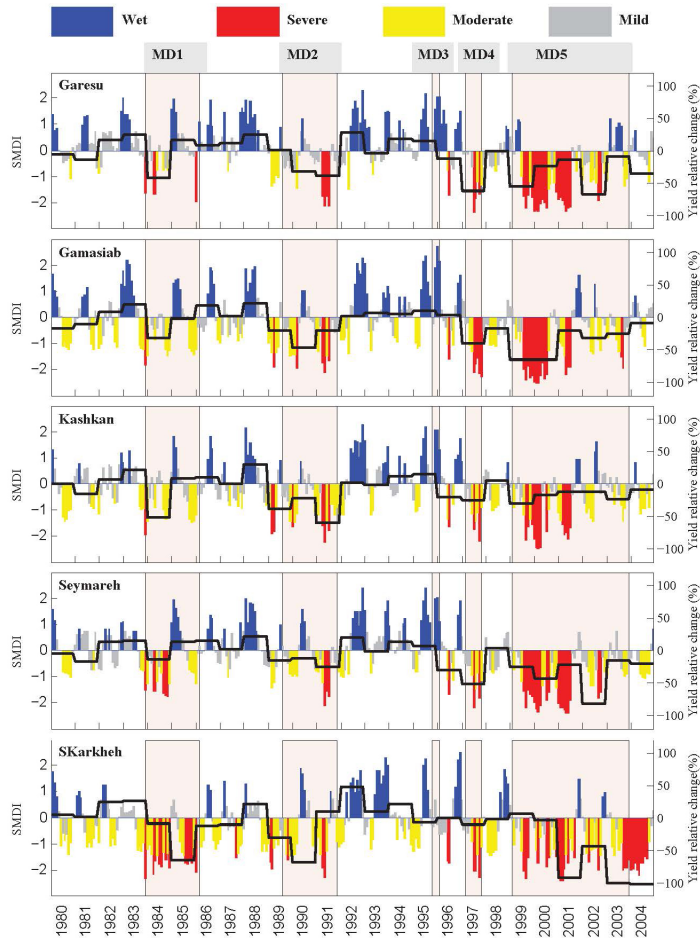


Figure 6. The time series of SMDI index in the five catchments during the period 1980–2004. The shaded bars highlight the five meteorological drought events (AD1–AD5).

Title Page

Abstract

Introduction

Conclusions

References

Tables

Figures

⏪

⏩

◀

▶

Back

Close

Full Screen / Esc

Printer-friendly Version

Interactive Discussion

Identification of spatiotemporal patterns of biophysical droughts in semi-arid region

B. Kamali et al.

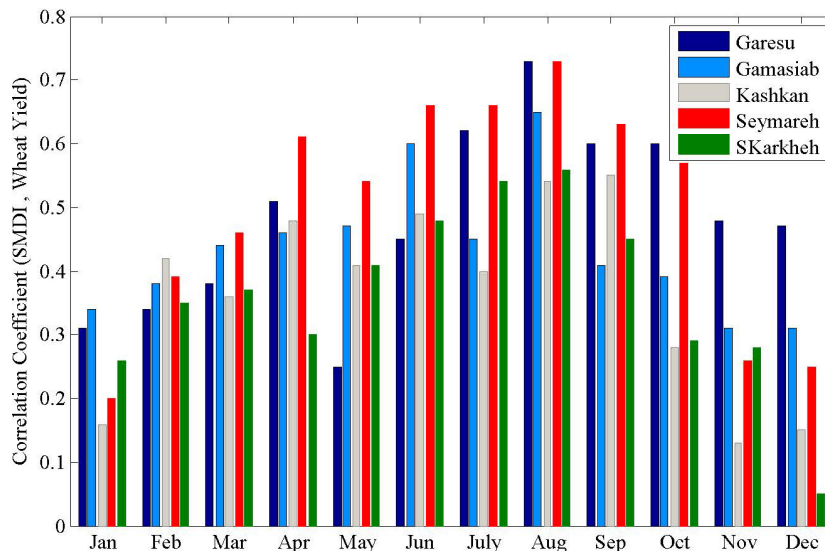


Figure 7. Correlation of monthly SMDI with relative changes in wheat yield in the five catchments of KRB.

Identification of spatiotemporal patterns of biophysical droughts in semi-arid region

B. Kamali et al.

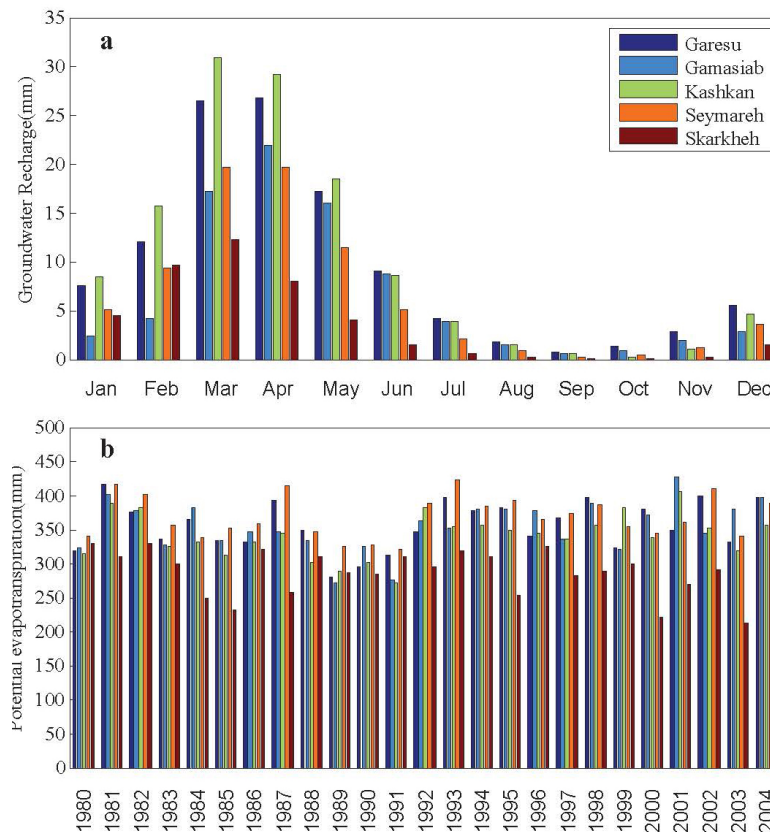


Figure 8. (a) Monthly time series of groundwater recharge values in the five catchments averaged over the studied period; (b) yearly potential evapotranspiration values in the five catchments during the studied period.